Keywords
Chikungunya–COVID-19 co-infection; Mathematical epidemiology; Nonlinear dynamical system; Intuitionistic fuzzy set; Uncertainty modelling; Enhanced Adaptive Fuzzy Membership Function; Stability analysis; Sensitivity analysis; Robustness

Authors
Vijayalakshmi G.M
Department of Mathematics, Vel Tech Rangarajan Dr. Sagunthala R & D Institute of Science and Technology, Avadi, Tamil Nadu, India - 600062,
ORCID ID: https://orcid.org/0000-0002-7475-242X,
Email id- drvijayalakshmi@veltech.edu.in

Vikram R
Department of Mathematics, Vel Tech Rangarajan Dr. Sagunthala R & D Institute of Science and Technology, Avadi, Tamil Nadu, India - 600062,
Department of Mathematics, DRBCCC Hindu College, Pattabiram,
Tamil Nadu, India - 600072,
ORCID ID: https://orcid.org/0009-0001-2754-7941,
Email id- rvikrammaths@gmail.com

Received:13-06-2026
Revised:17-07-2026
Accepted:28-07-2026
Doi:10.1922/ejprd.v34i7s.1672

European Journal of Prosthodontics and Restorative Dentistry (2026) 34 (7s), 554–571

An Intuitionistic Fuzzy Co-Infection Model for Chikungunya and COVID-19 Using Enhanced Adaptive Fuzzy Membership Functions

Abstract
This paper introduces a novel mathematical framework to study the co-infection dynamics of Chikungunya and COVID-19 under uncertainty. A nonlinear compartmental model is formulated using a system of ordinary differential equations incorporating saturated incidence, vaccination (with waning immunity), and recovery mechanisms. To overcome the limitations of deterministic approaches, an Enhanced Adaptive Fuzzy Membership Function (EAFMF), developed based on intuitionistic fuzzy set theory, is proposed to capture asymmetric uncertainty and hesitation in epidemiological parameters. The analysis includes the characterization of feasible regions, equilibrium points, and local stability through Jacobian-based eigenvalue analysis. Simulation results indicate that the deterministic model exhibits high sensitivity and oscillatory behaviour under increased transmission across multiple scenarios with baseline parameters. In contrast, the EAFMF-based model produces smoother dynamics, reduced infection peaks, and improved convergence stability. Sensitivity and robustness analyses further demonstrate that the proposed framework effectively moderates parameter perturbations. These findings highlight the importance of uncertainty-aware modelling for realistic epidemic prediction, and provide a robust framework for analysing complex co-infection systems.

INTRODUCTION

With the rise of emerging infectious diseases and their rapid spread around the world, there is an urgent need for comprehensive mathematical frameworks capable of understanding complex epidemiological dynamics. Specifically, the presence of multiple infectious diseases in a population poses substantial challenges for both modelling and public health intervention. The interplay of pathogens manifests in co-infection scenarios, in which individuals infected with one pathogen become susceptible to another, either coincident or subsequently (Anderson and May 1992), often resulting in nonlinear interactions that change transmission dynamics, recovery rates, and the persistence of infection. The recent pandemic of COVID-19 along with persistent vector-borne diseases such as Chikungunya highlights the significance of integrated model approaches in capturing such interactions.

Deterministic compartmental models form the backbone of mathematical epidemiology for analysing disease transmission and control strategies. These models have played a vital role in understanding threshold dynamics, equilibrium behavior, and stability conditions. Nevertheless, classical models frequently rely on the premise of precise parameter values, which may not accurately represent real-world epidemiological systems that inherently contain uncertainty, variability, and incomplete information about the population of interest. Within the context of diseases emerging and co-circulating, parameters like transmission rates, immunity efficacy, and recovery rates often exhibit a high level of uncertainty due to environmental variation, reporting delays, and population heterogeneity.

Recent studies have attempted to incorporate uncertainty into epidemiological models using probabilistic, stochastic, and fuzzy approaches. Fuzzy set theory is one of them, and it offers a flexible framework for representing vague and imprecise information. Especially, Intuitionistic fuzzy sets are a generalization of classical fuzzy models that allows for degrees of membership, non-membership, and hesitation; they provide a richer framework for dealing with uncertainty. However, existing fuzzy epidemic models are still mostly limited to symmetric membership functions, thus failing to adequately capture asymmetric uncertainty and parameter-dependent variability often present in co-infection systems.

A further limitation of previous works results from their limited integration of uncertainty modelling and rigorous dynamical systems analysis. Although dynamics of co-infection or fuzzy epidemic models in isolation have been extensively investigated, few research efforts have integrated these approaches with a comprehensive analysis of stability, eigenvalues and robustness. Additionally, the effect of uncertainty on qualitative features of epidemic systems (such as stability margins, oscillatory dynamics and convergence structures) is yet to be well understood.

In order to bridge these gaps, the current work proposes a novel Chikungunya and COVID-19 co-infection model with an EAFMF that combines nonlinear epidemiological dynamics. This framework provides an adaptive way to model the asymmetric uncertainty in epidemiological parameters while considering the hesitation effect through an intuitionistic fuzzy approach. This enables a more realistic and flexible representation of epidemiological uncertainty.

The model is formulated as a system of nonlinear ordinary differential equations with basic epidemiological mechanisms including saturation incidence, vaccination, immunity and waning immunity. We undertake a thorough analytical and numerical exploration with the identification of feasible regions, equilibrium points and local stability conditions based on Jacobian eigenvalue analysis. Furthermore, scenario-based simulations are conducted to investigate the impact of different transmission intensity and intervention strategies based on both deterministic (crisp) and uncertainty-driven (EAFMF) parameter values.

This work provides an important contribution in the comparison between crisp and EAFMF models. The study demonstrates that the proposed EAFMF framework significantly enhances system stability and robustness under parameter perturbations. Results of sensitivity and robustness analyses provide evidence for the predominance of key epidemiological parameters and validate the framework's ability to represent realistic disease dynamics under uncertainty.

The rest of the paper is organized as follows: The relevant literature pertaining to co-infection modelling and fuzzy epidemiologic approaches is found in Section 2. Section 3 presents the mathematical preliminaries and the EAFMF framework. Section 4 presents the co-infection model we propose. Sections 5 and 6 explore parameter settings and numerical simulations under the crisp assumption, while Section 7 extends the analysis within an EAFMF-based framework. Stability and sensitivity analysis are covered in Sections 8 and 9. The concluding section summarizes the main findings and contributions of the research.

2. Literature Review

Classical deterministic compartmental models have long formed the foundation of mathematical epidemiology which has long been used to explore the dynamics of disease transmission, equilibrium and stability properties. Seminal works laid the theoretical groundwork for epidemic modelling, introducing critical threshold concepts like the basic reproduction number (R_0), which dictates disease invasion and persistence in populations [1]–[5]. These have recently been expanded to model more complex nonlinear interactions as well as environmental drivers for a better fit of epidemic projections [6]. In particular, dynamical systems analyses of equilibrium and bifurcation theory have been used to study stability and qualitative behavior of such models [7], [8].

Since the emergence of COVID-19, many studies have been dedicated to exploring its transmission dynamics under diverse epidemiological settings. These include models that incorporate comorbidities, control measures and heterogeneous transmission dynamics for insights into disease spread and mitigation strategies [9]–[12]. Furthermore, models incorporating time-varying

parameters and fuzzy transitions have been proposed [13] to overcome underreporting and uncertainty in real data. Also, co-infection dynamics have been highlighted, illustrating the interplay between several pathogens and their joint contribution to disease burden [14].

An extensive body of work has focused on the study of vector-borne diseases like Chikungunya using non-linear dynamical models incorporating environmental variability, vector-host interactions and control strategies [15], [16]. Furthermore, the epidemiology of co-infecting diseases such as dengue and Chikungunya also reveal complex nonlinear transmission and immune interactions that may drive epidemic consequences [17]. Epidemiological and experimental studies have also contributed to our understanding of disease progression, as well as control mechanisms [18], [19]. In addition, global analyses of co-infection prevalence emphasize the utility of integrated modelling frameworks across multiple diseases [21].

An increasing application of fuzzy set theory has been widely observed in epidemiological modelling due to the uncertainties that are inherent to epidemiological data. The components of an intuitionistic fuzzy set, designed to incorporate membership, non-membership, and hesitancy degrees, was proposed to provide a more advanced representation of imprecision and uncertainty during parameters estimation [22]. The basis of fuzzy arithmetic and differential equations (DE) [23], [24] have enabled the incorporation of uncertainty in dynamical systems, while advanced extensions of the fuzzy set theory provide more flexibility for modelling solutions [25]. Indeed, these methods have been applied successfully to epidemic systems [26], [27], providing solution approximations which are more realistic than classical deterministic model output.

In the recent studies, hybrid fuzzy epidemic models were investigated which in most cases have been generated for COVID-19 with better numerical stability and predictive capability [28], [29]. As it relates to vaccination strategies, control measures, and decision-making processes, integrating fuzzy uncertainty in epidemic dynamics has improved upon the realism encompassed within these modelling efforts [30], [31]. Furthermore, fuzzy and fractional-order epidemic models have been proposed, which can capture memory effects and complex transmission mechanisms with stronger descriptive ability [32], [33].

Building upon these advances, recent works have stressed the importance of adaptive and robust uncertainty modelling techniques. To overcome these limitations, recent studies have proposed approaches to capture asymmetric uncertainty and hesitation effects with improved granularity using an Enhanced Adaptive Fuzzy Membership Function (EAFMF) framework [34]–[37]. Numerical methods for solving nonlinear differential equations are still the basis for validating such models and ensuring computational accuracy [38]. Furthermore, studies on parameter estimation and sensitivity analysis are also important to characterize the impact of model parameters and test robustness under uncertainty [39]–[41]. The applicability of mathematical tools to complex real-world situations can be further extended through birth-death models [41], and several emerging trends such as fractional order and nonlocal epidemic models [42], [43].

Nonetheless, most existing models do not jointly account for co-infection dynamics and asymmetric uncertainty in a single framework. This gap drives the current study, which simultaneously integrates EAFMF-based intuitionistic fuzzy modelling and nonlinear co-infection dynamics to provide a more coherent and realistic representation of co-infection dynamics.

3. Mathematical Preliminaries and Definitions

This section lays the groundwork for the mathematical theory underlying EAFMF development for equilibrium analysis, stability analysis, sensitivity analysis and uncertainty modelling.

Definition 3.1. Feasible Region

Define $\Omega = \{(S, I, C, R_1, R_2) \in \Re_+^5 : S + I + C + R_1 + R_2 \leq K\}$. If all trajectories projected from points in Ω remain in Ω for all $t \geq 0$, we say that the region Ω is positively invariant.

This guarantees solutions that are biologically feasible, bounded and non-negative.

Definition 3.2. Equilibrium Point

An equilibrium point $E^*=(S^*, I^*, C^*, R_1^*, R_2^*)$ satisfies

$$\frac{dS}{dt}=\frac{dI}{dt}=\frac{dC}{dt}=\frac{dR_1}{dt}=\frac{dR_2}{dt}=0$$

From this we discussed about two kinds of equilibria.

- Disease-Free Equilibrium (DFE): $(I^*=C^*=0)$
- Endemic (Interior) Equilibrium: all elements positive

These equilibria define criteria for disease extinction or persistence.

Definition 3.3. Local Stability via Jacobian Matrix

For the model, let $J(E^*)$ as the Jacobian matrix of the system evaluated at equilibrium (E^*).

We denote the eigenvalues of $J(E^*)$ by λ_i , $i = 1,2,\ldots,n$.

The equilibrium E^* is:

- Locally asymptotically stable if: $\mathrm{Re}(\lambda_i)<0$, for all i..
- Unstable if: there exists i, such that , $Re(\lambda_i)>0$.

Real parts of eigenvalues represent the margin of stability and rate of convergence.

Definition 3.4 (Normalized Sensitivity Measure)

Let X be a model output and p be a parameter. The normalized forward sensitivity index is defined by

$$\Gamma_p^X = \frac{\partial X}{\partial p} \cdot \frac{p}{X}$$

The secondary contribution builds on the index, which quantifies the relative effect of parameter perturbation to guide perturbation-based robustness analysis for a model.

Definition 3.5. Intuitionistic Fuzzy Set
For a universe of discourse X, let A be an Intuitionistic Fuzzy Set (IFS) defined as $A = \{(x,u_A(x),v_A(x)) \mid x \in X\}$, where $u_A(x)$: membership function, $v_A(x)$: non-membership function, $0 \le u_A(x) + v_A(x) \le 1$.

The degree of hesitancy is $\pi(x) = 1 - u_A(x) - v_A(x)$ measuring remaining uncertainty.

Definition 3.6. Enhance Adaptive Fuzzy Membership Function (EAFMF)
For a parameter $x \in [p_{Lb}, p_{Ub}]$, the EAFMF can be defined as

$$u(x) = \begin{cases} 0, & x < p_{Lb} \\ \frac{x - p_{Lb}}{p_{mid} - p_{Lb}}, & p_{Lb} \le x \le p_{mid} \\ 1, & p_{mid} < x \le p'_{mid} \\ \frac{1 - \frac{x - p'_{mid}}{p_{Ub} - p'_{mid}}}{2}, & p'_{mid} < x \le p_{Ub} \\ 0, & x > p_{Ub} \end{cases}$$

where, $p_{mid} = \frac{2p_{Lb} + p_{Ub}}{3}$ and $p'_{mid} = \frac{p_{Lb} + 2p_{Ub}}{3}$

Definition 3.7. Adaptive Raw Non-Membership and Non-Membership Function
The raw non-membership function is given by

$$R_v(x) = \begin{cases} 1, & x < p_{Lb} \\ \frac{p'_{mid} - x}{p'_{mid} - p_{Lb}}, & p_{Lb} \le x \le p'_{mid} \\ 0, & p'_{mid} < x \le p_{Ub} \\ \frac{x - p_{Ub}}{p_{Ub} - p'_{mid}}, & x > p_{Ub} \end{cases}$$

Then the non-membership is, $v(x) = R_v(x) \times (1 - u(x))$

Definition 3.8. Adaptive Centroid Defuzzification
With the weighted intuitionistic centroid that considers asymmetric uncertainty, hesitation and interval-based importance simultaneously, the intuitionistic fuzzy parameter is translated into crisp value. The defuzzification is given by:

$$z^* = \frac{\int_x x \cdot [u(x) - v(x)][1 - \pi(x)] w(x)\, dx}{\int_x [u(x) - v(x)][1 - \pi(x)] w(x) dx}$$

where $w(x)$ is the LB–UB-driven adaptive weighting function defined by.

$$w(x) = \frac{x - p_{Lb}}{p_{Ub} - p_{Lb}}$$

4. Mathematical Model formulation:
The proposed work consists of a co-infection model that describes the temporal evolution of a human population affected by Chikungunya and COVID-19 through a system of nonlinear ordinary differential equations. The following notations are used to denote state variables and model parameters that drive disease transmission, recovery, vaccination, immunity and waning of immunity in the population.

4.1. Variables:
$S(t)$: Susceptible individuals (healthy individuals who can be infected with Chikungunya or COVID-19).

- $I(t)$: Chikungunya-infected population (a population with high risk of COVID-19 infection)
- $C(t)$: COVID-19-infected individuals.
- $R_1(t)$: Individuals recovered from COVID-19 infection originating from the Susceptible class
- $R_2(t)$: Individuals recovered from COVID-19 infection originating from Chikungunya-infected class.

4.2. Parameters:

- k: Transmission rate of Chikungunya infection.
- K: Carrying capacity of the total population
- e_1, e_2: Conversion efficiencies associated with COVID-19 transmission from susceptible individuals and Chikungunya-infected individuals.
- a_1, a_2: Rates of COVID-19 infection in susceptible and Chikungunya-infected individuals.
- h_1, h_2: Saturation parameters representing nonlinear incidence effects and reduced transmission efficiency at higher population levels.
- d_C: Natural decay rate of COVID-19 virus.
- g: Growth rate of susceptible individuals (through birth or immigration)
- r_1: Recovery rate of people with COVID-19 from susceptible population.
- r_2: Recovery rate of COVID-19-infected individuals from Chikungunya-infected population.
- v: The vaccination rate of both susceptible and Chikungunya-infected population
- i_1, i_2: Immunity of naive and Chikungunya-infected individuals
- w_1, w_2: Rates of waning immunity for $R_1(t)$ and $R_2(t)$.

All parameters are assumed to be non-negative to ensure biological feasibility of the model.

4.3. Mathematical Model:
The dynamics of the Chikungunya–COVID-19 co-infection are modelled by the following system of nonlinear ordinary differential equations

4.3.1. Susceptible Individuals (S(t)):

$$\frac{dS}{dt}=gS\left(1-\frac{S+I+R_1+R_2}{K}\right)-kSI-\frac{a_1SC}{1+a_1h_1S}-vS+w_1R_1+w_2R_2$$

4.3.2. Chikungunya-Infected Individuals (I(t)):

$$\frac{dI}{dt}=kSI-\frac{a_2IC}{1+a_2h_2I}-vI$$

4.3.3. COVID-19-Infected Individuals (C(t)):

$$\frac{dC}{dt}=\frac{e_1a_1SC}{1+a_1h_1S}+\frac{e_2a_2IC}{1+a_2h_2I}-d_CC$$

4.3.4. Recovered S(t) Individuals ($R_1(t)$):

$$\frac{dR_1}{dt}=r_1i_1\frac{a_1SC}{1+a_1h_1S}+vS-w_1R_1$$

4.3.5. Recovered I(t) Individuals ($R_2(t)$):

$$\frac{dR_2}{dt}=r_2i_2\frac{a_2IC}{1+a_2h_2I}+vI-w_2R_2$$

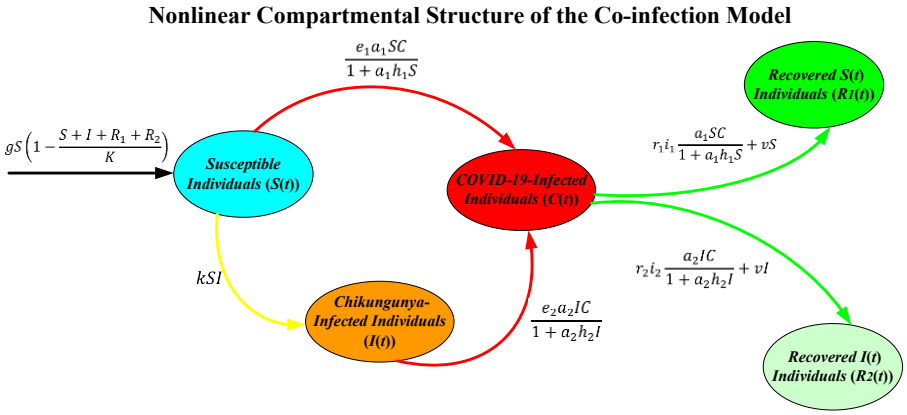

Figure 1: Compartmental structure of the nonlinear Chikungunya–COVID-19 co-infection model incorporating saturated incidence, vaccination, and recovery mechanisms.

4.4. Key Dynamics of the Model

This model describes the dynamics of a population affected by two interacting diseases: Chikungunya and COVID-19, through transitions between five compartments. Also, it uses a system of differential equations to incorporate important processes such as disease transmission, vaccination, immunity and waning immunity.

S equation: susceptible population increase due to natural growth gS and immunity loss from the recovered classes $w_1R_1+w_2R_2$, while it decreases due to Chikungunya transmission kSI, COVID-19 infection $\frac{a_1SC}{1+a_1h_1S}$ and vaccination vS. The class infected with Chikungunya may increase from kSI transmission and decrease as they become exposed to COVID-19 $\frac{a_2IC}{1+a_2h_2I}$ and by vaccination vI, due to their increased susceptibility under co-infection. Saturated incidence terms accounting for infections from both susceptible and Chikungunya-infected population drive COVID-19 dynamics, with natural decay d_CC governing persistence. Recovery classes increase due to COVID-19 recovery $r_1i_1\frac{a_1SC}{1+a_1h_1S}, r_2i_2\frac{a_2IC}{1+a_2h_2I}$ and vaccination, but decrease due to waning immunity $w_1R_1+w_2R_2$. Such feedbacks allow recurrent outbreaks and sustained coexistence of infections.

4.5. Key Modelling Assumptions

- $a_2 > a_1$: Chikungunya-infected persons are at greater risk of COVID-19.
- $e_2 > e_1$: COVID-19 spreads more effectively from co-infected hosts
- $(r_2 < r_1)$: Recovery is slower under co-morbidity.
- $(w_2 > w_1)$: Immunity wanes faster in previously co-infected individuals.

These assumptions are in agreement with the clinical and epidemiological data that have been reported regarding Chikungunya co-infection, immune balance disruption and chronic disease burden [16], [17], [21].

5. Reason for Parameter Selection and Ranges

Because reliable datasets characterizing concurrent COVID-19–Chikungunya co-circulation are not available in real time, input parameters were chosen from biologically plausible values described in the established peer-reviewed literature on vector-borne diseases, COVID-19 transmission dynamics, and comorbidity modelling.

Parameters for transmission and interaction were derived from valid epidemic models, which included nonlinear incidence, population constraints, and saturation effects [1], [2], [9], [10] to best model realistic mechanisms through which disease spreads. Parameters determining vulnerability and recovery were selected based on increased susceptibility/delayed recovery attributable to co-infection [10], [16], [17].

The parameters corresponding to vaccination and immunity were calculated using theoretical studies of vaccination and immunity, which aim to ensure epidemiologic realism rather than policy-specific calibration [13], [43]. Declining immunity rates were incorporated as per factual immune decay and reinfection patterns from recent epidemic modelling studies [13], [18].

ll parameters are assumed to be positive, bounded and satisfy feasibility conditions required for equilibrium and stability. Furthermore, the Enhanced Adaptive Fuzzy Membership Function (EAFMF) systematically accounts for uncertainty by adjusting its parameter values within biologically plausible ranges, thereby improving the robustness and time-consistency of qualitative model predictions in the presence of uncertainty.

5.1. Parameter Values Used in Simulations

Table 1: Model Parameters, Baseline Values, Ranges, and Literature Sources

Parameter	Description	Value Used	Range	Reference
(k)	Chikungunya transmission rate	0.0020	0.001–0.010	[15], [16], [17]
(K)	Carrying capacity	2000	1000–5000	[1], [2]
(e_1)	Conversion efficiency (S → C)	0.4000	0.200–0.600	[10], [129]
(e_2)	Conversion efficiency (I → C)	0.6000	0.300–0.800	[10], [29]
(a_1)	COVID-19 infection rate (S)	0.0015	0.001–0.010	[9], [10], [30]
(a_2)	COVID-19 infection rate (I)	0.0030	0.002–0.020	[9], [10], [30]
(h_1)	Saturation parameter (S)	0.1000	0.050–0.500	[9], [28]
(h_2)	Saturation parameter (I)	0.1500	0.050–0.700	[9], [28]
(d_C)	COVID-19 decay rate	0.2000	0.100–0.500	[9], [10]
(g)	Population growth rate	0.0100	0.005–0.030	[1], [2]
(r_1)	COVID-19 recovery rate (S)	0.1500	0.100–0.250	[9], [10]
(r_2)	COVID-19 recovery rate (I)	0.1000	0.050–0.200	[9], [10]
(v)	Vaccination rate	0.5000	0.100–2.000	[21], [37], [43]
(i_1)	Immunity strength (S)	0.8000	0.600–1.000	[22], [27]
(i_2)	Immunity strength (I)	0.6000	0.400–0.900	[22], [27]
(w_1)	Waning immunity (R_1)	0.0100	0.005–0.050	[13], [37]
(w_2)	Waning immunity (R_2)	0.0150	0.005–0.060	[13], [37]

5.2. Constraints on state variables and initial conditions

For every state variable, the carrying capacity K remains the limit on total population. The initial values chosen were consistent with the co-circulation scenario early in the epidemic where a large proportion of the population remains susceptible to both pathogens, and both COVID-19 and Chikungunya are circulating at low-to-moderate rates.

5.3. Carrying Capacity

To ensure known bounds and mathematical manageability of solutions, we adapt the carrying capacity K=2000, a well-defined normalised closed population in theoretical epidemic modelling.

5.4. Initial Conditions and State Variable Values

Table 2: Initial Conditions and Justification for the Co-infection Model Simulations

Variable	Description	Initial Value	Justification	Reference
$(S(0))$	Susceptible individuals	1200	Majority initially healthy	[1], [2]
$(I(0))$	Chikungunya-infected individuals	500	Endemic vector-borne presence	[15], [16], [18]
$(C(0))$	COVID-19 infected individuals	100	Early-stage COVID-19 exposure	[9], [10], [30]
$(R_1(0))$	Susceptible individuals recovered from COVID-19	150	Partial recovery after infection	[9], [10]
$(R_2(0))$	Chikungunya-infected individuals recovered from COVID-19	50	Smaller recovered co-infected class	[9], [17]

$$S(0)+I(0)+C(0)+R_1(0)+R_2(0) = 1200+500+100+150+50=2000=K$$

5.5. Justification

5.4.1. Verification of Carrying Capacity Constraint

The chosen parameter values and initial conditions ranged within biologically plausible scope based on previously reported estimates for COVID-19, vector-borne diseases, and co-infection dynamics. As real-time data on COVID-19–Chikungunya co-circulation is currently limited, the parameters were calibrated to yield epidemiologically consistent, positive and bounded solutions. Population distributions at the outset are representative of early-stage co-circulation, in which Chikungunya is treated as endemic, and COVID-19 is introduced (at low prevalence), mirroring previous modelling efforts [9], [15], [16], [18].

6. Numerical Simulations and Scenario-Based Parameter Analysis for Crisp Values

Here we present numerical simulations of the COVID-19–Chikungunya in the framework of distinct epidemiological transmission and intervention scenarios. Since no reliable real-time datasets are available describing simultaneous COVID-19–Chikungunya co-circulation, simulations using biologically plausible parameter regimes are performed to assess qualitative system behaviour and intervention efficacy.

Only selected parameters are varied across scenarios to investigate the influence of transmission intensity and control strategies. In particular, parameters including rates of infection (a_1, a_2), saturation parameters (h_1, h_2), the viral decay rate d_C, recovery rates (r_1, r_2), vaccination rate v, immunity strength (i_1, i_2) and waning immunity periods (w_1, w_2) are varied to analyse their influence on the system dynamics. These parameters mainly control infection pressure, recovery dynamics, immunity persistence and public health intervention strength.

Other structural parameters are constant, including the Chikungunya transmission rate k; carrying capacity K; and conversion efficiencies (e_1, e_2), allowing us to isolate the role of COVID-19 transmission heterogeneity and intervention mechanisms. This approach ensures meaningful comparison across scenarios while maintaining biological plausibility.

The setup of the scenario-specific parameters is summarized in Table 3.

Table 3: Scenario-based parameter settings for crisp simulation

Parameter	Case I: Baseline	Case II: High COVID Transmission	Case III: Improved Immunity & Vaccination	Case IV: High Transmission + Control
(k)	0.002	0.002	0.0020	0.002
(K)	2000	2000	2000	2000
(a_1)	0.0015	0.015	0.0015	0.015
(a_2)	0.0030	0.030	0.0030	0.030
(h_1)	0.1000	0.200	0.1000	0.200
(h_2)	0.1500	0.250	0.1500	0.250
(d_C)	0.2000	0.100	0.5000	0.500
(r_1)	0.1500	0.150	0.2500	0.250
(r_2)	0.1000	0.100	0.2000	0.200
(v)	0.5000	0.500	0.8000	0.800
(i_1)	0.8000	0.800	0.9000	0.900
(i_2)	0.6000	0.600	0.8000	0.800
(w_1)	0.0100	0.100	0.0100	0.100
(w_2)	0.0150	0.150	0.0150	0.150

Figures 2.1 – 2.4 represents the diagrammatic representations corresponding to the four scenarios.

(i) Baseline co-circulation dynamics

(ii) Intensified COVID-19 transmission

(iii) Improved recovery due to better immunity and vaccination

(iv) Resilience of interventions against high transmission pressure

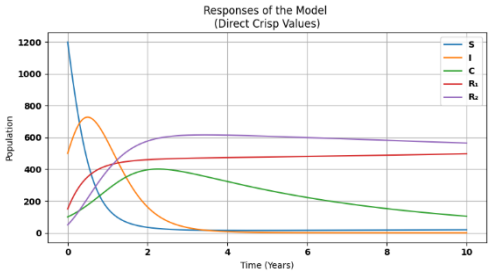

Fig.2.1: Baseline co-circulation dynamics (Crisp Values)

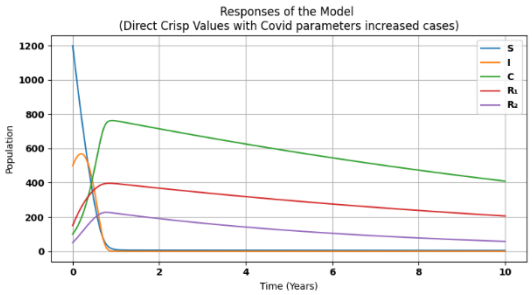

Fig.2.2: Intensified COVID-19 transmission Scenario

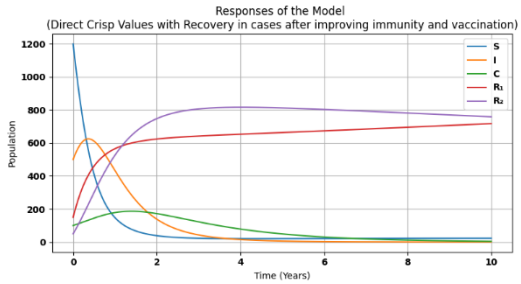

Fig. 2.3: Enhanced recovery through improved immunity and vaccination

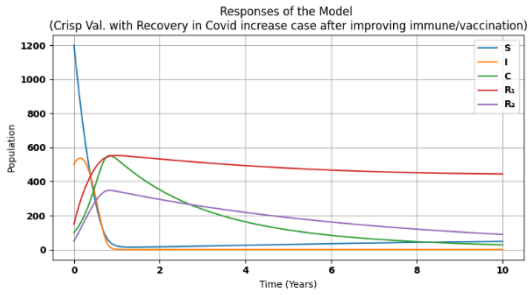

Fig. 2.4: High Transmission with Strengthened Intervention

These controlled variations allow for systematic assessment of infection amplification, recovery facilitation and robustness of intervention before implementing uncertainty-competent fuzzy analysis.

6.1. Results and Discussion of crisp simulations

The results of the simulation under the four epidemiological situations are described in Figs. 2.1–2.4.

6.1.1. Baseline Scenario (Fig. 2.1.)

The dynamics here are characterized by stable co-circulation of the two systems. The COVID-19 infections rise initially and later on declines owing to recoveries and natural decay, while Chikungunya remains at moderate endemic levels. In this initial outbreak phase, the susceptible population decreases and becomes more stable as recovered class continues to grow.

6.1.2. High Transmission Scenario (Fig. 2.2.)

Increased infection rates (a_1,a_2) drastically increases COVID-19 incidence, resulting in higher peaks and a more rapid decline of susceptible individuals. The delay before stabilization compared to the baseline case again underscores the sensitivity of the system to transmission intensity.

6.1.3. Improved Immunity and Vaccination Scenario (Fig. 2.3.)

Increased vaccination rates (v), along with improved immunity (i_1, i_2) and recovery rates (r_1,r_2) markedly decrease peaks in the number of infections, while enhancing recovery. This shows their dominance over the recovered classes and therefore indicates that those infections do not trigger an epidemic.

6.1.4. With respect to control: High Transmission Scenario (Fig. 2.4.)

Even in the face of increased transmission pressure, enhanced vaccination and immune enhancement reduce chronicity. While initial infection peaks are significant, the system ultimately stabilizes with sustained intervention strategies suggesting robust resilience.

6.2. Overall Interpretation of Crisp Simulations

The simulation results show that epidemic outcomes are highly sensitive to parameters related to transmission, recovery, and immunity. Infection rates have a small effect on how big the outbreak turns out and how long it takes to stabilize. Deterministic models, however, depend on fixed parameter values that in reality may vary quite a bit within the epidemiological context.

This limitation motivates extending the current framework to a modelling approach that is sensitive to uncertainty, i.e., leveraging the Enhanced Adaptive Fuzzy Membership Function (EAFMF), coupled with an effective adaptive sequential process which increasingly leverages asymmetric uncertainties and hesitancy effects in transmission and recovery parameters.

7. AFMF-Based Uncertainty Modelling

7.1 EAFMF-Based Intuitionistic Fuzzification Results

7.1.1 EAFMF Computation for the Sample Parameter Set

In order to showcase the implementation of the proposed Enhanced Adaptive Fuzzy Membership Function (EAFMF) a typical epidemic parameter has been considered. The rate of Chikungunya transmission k is a parameter chosen due to the significant uncertainty with which it has been reported in the literature.

The nominal value is:

$$x = 0.002$$

with uncertainty interval:

$$[p_{Lb}, p_{Ub}] = [0.001, 0.01]$$

The asymmetric transition parameters are computed according to the EAFMF formulation:

$$p_{mid} = \frac{2p_{Lb} + p_{Ub}}{3} = \frac{2(0.001) + (0.01)}{3} = 0.004,$$

$$p'_{mid}=\frac{p_{Lb}+2p_{Ub}}{3}=\frac{(0.001)+2(0.01)}{3}=0.007$$

Since $p_{Lb}\le x\le p_{mid}$, the degree of membership is:

$$u(x)=\frac{x-p_{Lb}}{p_{mid}-p_{Lb}}$$

$$=\frac{0.002-0.001}{0.004-0.001}$$

$$=0.333.$$

The raw non-membership degree is:

$$R_{v(x)}=\frac{p'_{mid}-x}{p'_{mid}-p_{Lb}}$$

$$=\frac{0.007-0.002}{0.007-0.001}$$

$$=0.833$$

Based on the EAFMF definition, the effective degree of non-membership is modified with the membership value,

$v(x) = R_{v(x)}[1 - u(x)] = 0.833\ (1 - 0.333) = 0.556.$

The hesitation degree is:

$\pi(x) = 1 - u(x) - v(x) = 1 - 0.333 - 0.556 = 0.111.$

This proves that the proposed EAFMF simultaneously captures:

- Partial membership
- Partial non-membership
- Explicit hesitation

All the other parameters undergo a similar process. Then, the resulting intuitionistic fuzzy representations are defuzzified based on the weighted intuitionistic centroid scheme.

Table 4. Representations and defuzzified values with intuitionistic fuzziness

Parameter	Lower Bound	Upper Bound	Nominal Value	Membership u(x)	Raw Non-Membership (R_v(x))	Adjusted Non-membership v(x)	Hesitation π_X	Defuzzified Value
(k)	0.001	0.01	0.0020	0.333	0.833	0.556	0.111	0.005667
(K)	1000	5000	2000.0000	0.750	0.625	0.156	0.094	3074.074074
(e_1)	0.200	0.60	0.4000	1.000	0.250	0.000	0.000	0.407407
(e_2)	0.300	0.80	0.6000	1.000	0.100	0.000	0.000	0.559259
(a_1)	0.001	0.01	0.0015	0.167	0.917	0.764	0.069	0.005667
(a_2)	0.002	0.02	0.0030	0.167	0.917	0.764	0.069	0.011333
(h_1)	0.050	0.50	0.1000	0.333	0.833	0.556	0.111	0.283333
(h_2)	0.050	0.70	0.1500	0.462	0.769	0.414	0.124	0.387037
(d_C)	0.100	0.50	0.2000	0.750	0.625	0.156	0.094	0.307407
(g)	0.005	0.03	0.0100	0.600	0.700	0.280	0.120	0.017963
(r_1)	0.100	0.25	0.1500	1.000	0.500	0.000	0.000	0.177778
(r_2)	0.050	0.20	0.1000	1.000	0.500	0.000	0.000	0.127778
(v)	0.001	0.02	0.0050	0.632	0.684	0.252	0.116	0.010852
(i_1)	0.600	1.00	0.8000	1.000	0.250	0.000	0.000	0.807407
(i_2)	0.400	0.90	0.6000	1.000	0.400	0.000	0.000	0.659259
(w_1)	0.005	0.05	0.0100	0.333	0.833	0.556	0.111	0.028333
(w_2)	0.005	0.06	0.0150	0.545	0.727	0.331	0.124	0.033519

7.2. Numerical Simulations Using EAFMF-Adjusted Parameters

In this section, numerical simulations of the proposed Chikungunya–COVID-19 co-infection model are conducted using corresponding defuzzified parameters using the EAFMF framework. These parameter values propagate asymmetric uncertainty and hesitation effects which are not captured in the deterministic (crisp) simulations.

To determine the effect of uncertainty-adjusted parameters, we analyse four epidemiological scenarios analogous to those in the crisp analysis:

- Baseline co-circulation
- High COVID-19 transmission
- Improved immunity and vaccination
- High transmission with strengthened intervention

The rates of COVID-19 infection (a_1,a_2), saturation parameters (h_1,h_2), rate of decay d_C, recovery rates (r_1,r_2), the vaccination rate v, the strength of immunity

(i_1,i_2), and waning immunity (w_1,w_2) are altered by utilizing their defuzzified values.

The structural parameters k,K,e_1,e_2, although uncertain (given the uncertainty about their values), do not vary between scenarios, to allow for consistent comparative analysis.

The defuzzified parameter configurations are presented in Table 5.

Table 5. EAFMF Framework: Scenario Based Defuzzified Parameter Settings

Parameter	Case I: Baseline (Defuzzified)	Case II: High COVID Transmission (Defuzzified)	Case III: Improved Immunity & Vaccination (Defuzzified)	Case IV: High Transmission + Control (Defuzzified)
(k)	0.005667	0.005667	0.005667	0.005667
(K)	3074.074074	3074.074074	3074.074074	3074.074074
(e_1)	0.407407	0.407407	0.407407	0.407407
(e_2)	0.559259	0.559259	0.559259	0.559259
(a_1)	0.005667	0.008963	0.005667	0.008963
(a_2)	0.011333	0.017926	0.011333	0.017926
(h_1)	0.283333	0.346667	0.283333	0.346667
(h_2)	0.387037	0.462963	0.387037	0.462963
(d_C)	0.307407	0.185185	0.444444	0.444444
(g)	0.017963	0.017963	0.017963	0.017963
(r_1)	0.177778	0.177778	0.233333	0.233333
(r_2)	0.127778	0.127778	0.177778	0.177778
(v)	0.632000	0.632000	0.781333	0.781333
(i_1)	0.807407	0.807407	0.874074	0.874074
(i_2)	0.659259	0.659259	0.733333	0.733333
(w_1)	0.028333	0.092593	0.028333	0.092593
(w_2)	0.033519	0.111111	0.033519	0.111111

The simulation results for were demonstrated in Figs. 3.1–3.4, representing:

Table 6: Diagrammatic representations corresponding to the four scenarios

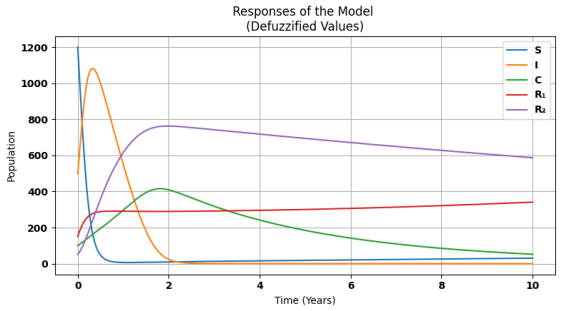

Fig.3.1: Baseline Co-circulation Dynamics under Defuzzified (EAFMF) Parameters

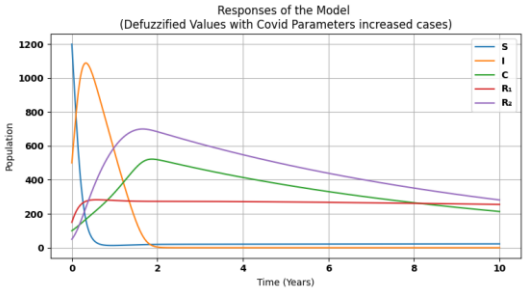

Fig.3.2: Intensified COVID-19 Transmission under Defuzzified Parameters

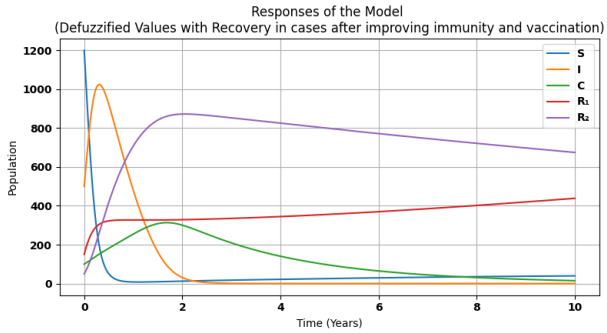

Fig.3.3: Enhanced Recovery through Improved Immunity and Vaccination (EAFMF Model)

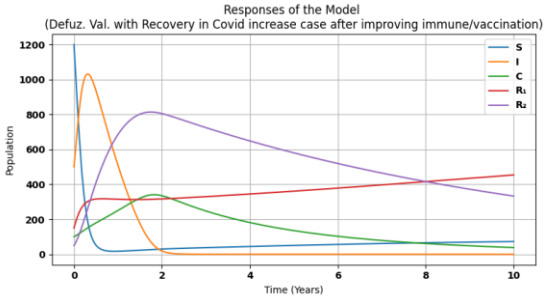

Fig.3.4: High Transmission with Strengthened Control under EAFMF Framework

(i) Time evolution of the co-infection system under baseline defuzzified parameters obtained by EAFMF framework

(ii) System response to higher COVID-19 transmission rates using EAFMF-adjusted parameters.

(iii) Effect of enhanced immunity and vaccinations under defuzzified parametric configurations.

(iv) The system response during high transmission pressure and the enhanced intervention when working with defuzzified parameters.

7.3. Results and Discussion of Simulations with EAFMF

Our new EAFMF-based adjusted parameter sets give rise to the system behaviour depicted in Figs. 3.1–3.4.

7.3.1. Baseline Fuzzy Scenario (Fig. 3.1.)

Relative to the crisp baseline, the model has smoother co-circulation dynamics. Peaks of infections are mitigated and convergence to equilibria is more gradual and stable. This represents balanced integration of transmission and recovery uncertainty.

7.3.2. High Transmission Scenario (Fig. 3.2.)

Infection rates (a_1, a_2) are higher, and COVID-19 prevalence increases moderately; but the trajectory of the outbreak is less sharp than in the crisp case. The reduced extreme oscillations suggest that numerical stability has been improved with respect to uncertainty on the parameter set.

7.3.3. Improved Immunity Scenario (Fig. 3.3.)

Vaccination v, immunity (i_1, i_2), and recovery rates (r_1, r_2) are enhanced to significantly dampen infection peaks and hasten stabilization. Recovery dominance seems to be smoother and less oscillatory than in the deterministic case.

7.3.4. High Transmission with Control (Fig. 3.4)

Even in conditions of high transmission pressure, intensified interventions substantially decrease the long-term burden of disease. The overall system displays better stability in terms of balancing and less reaction to parameter build up.

7.4. Overall Interpretation of EAFMF Simulations

EAFMF-based simulations indicate that the integration of intuitionistic fuzzy uncertainty leads to:

- Smoother epidemic trajectories
- Reduced amplification of infection peaks
- Improved convergence stability
- Decreased oscillatory behaviour
- Enhanced robustness under parameter variation

Crisp simulations use fixed point estimates, but the EAFMF framework incorporates asymmetric epistemic uncertainty between views and hesitancy on these views through parameter representation to obtain more realistic and reliable epidemic forecasts under real-world variability.

8. Plotting 3D Phase-Space Comparison in Equilibrium and Stability Analysis

This section analyses the equilibrium structure and local stability characteristics of the proposed Chikungunya–COVID co-infection model. We derive analytical stability conditions for crisp and EAFMF-adjusted parameter regimes respectively followed by three-dimensional phase-space visualization in order to assess convergence behaviour.

8.1 Positivity and Feasible Region

Let $\Omega = \{ (S,I,C,R_1,R_2) \in \mathcal{R}_+^5 : S+I+C+R_1+R_2 \leq K \}$

For positive initial conditions and parameters that are biologically reasonable, solutions stay non-negative and remain in the region Ω. So, the model is well-posed epidemiologically.

8.2 Disease-Free Equilibrium (DFE)

The Disease-Free Equilibrium (DFE) is relevant to active infection:

$$E_0 = (S^*, 0, 0, R_1^*, R_2^*)$$

Where S^* depends on vaccination and recovery dynamics. In the absence of vaccination and waning effects, this reduces to

$$E_0 = (K, 0, 0, 0, 0)$$

8.2.1. Stability Condition

The DFE is locally asymptotically stable if the effective reproduction number satisfies:

$$R_0 < 1$$

where R_0 depends primarily on transmission parameters:

- k
- a_1, a_2
- e_1, e_2
- Although deriving an explicit closed-form expression of R_0 is analytically challenging due to nonlinear incidence terms, it can be conceptually characterised using the next-generation matrix framework based on transmission and recovery parameters.

Under crisp parameters, larger infection coefficients increase R_0, potentially destabilizing the DFE.

Under EAFMF-adjusted parameters, transmission rates are moderated, reducing instability risk.

8.3 Interior (Endemic) Equilibrium

An interior equilibrium

$$E^* = (S^*, I^*, C^*, R_1^*, R_2^*)$$

satisfies:

$$\frac{dS}{dt}=\frac{dI}{dt}=\frac{dC}{dt}=\frac{dR_1}{dt}=\frac{dR_2}{dt}=0$$

with all components positive.

The existence of E^* requires:

$$R_0>1$$

ensuring sustained disease persistence.

8.4 Jacobian Matrix and Local Stability

Denote the Jacobian matrix evaluated at equilibrium as $J(E^*)$. The characteristic equation is:

$$\left|J(E^*)-\lambda I\right|=0$$

The equilibrium is locally asymptotically stable if:

$$Re(\lambda_i)<0 \text{ ,for all } i$$

For simulation, the model equations are represented as

$$f_1=\frac{dS}{dt}=gS\left(1-\frac{S+I+R_1+R_2}{K}\right)-kSI-\frac{a_1SC}{1+a_1h_1S}-vS+w_1R_1+w_2R_2$$

$$f_2=\frac{dI}{dt}=kSI-\frac{a_2IC}{1+a_2h_2I}-vI$$

$$f_3=\frac{dC}{dt}=\frac{e_1a_1SC}{1+a_1h_1S}+\frac{e_2a_2IC}{1+a_2h_2I}-d_CC$$

$$f_4=\frac{dR_1}{dt}=r_1i_1\frac{a_1SC}{1+a_1h_1S}+vS-w_1R_1$$

$$f_5=\frac{dR_2}{dt}=r_2i_2\frac{a_2IC}{1+a_2h_2I}+vI-w_2R_2$$

At equilibrium point $E^*=(S^*, I^*, C^*, R_1^*, R_2^*)$, the Jacobian matrix of the system is defined as

$$J=\begin{bmatrix}\frac{\partial f_1}{\partial S} & \frac{\partial f_1}{\partial I} & \frac{\partial f_1}{\partial C} & \frac{\partial f_1}{\partial R_1} & \frac{\partial f_1}{\partial R_2}\\ \frac{\partial f_2}{\partial S} & \frac{\partial f_2}{\partial I} & \frac{\partial f_2}{\partial C} & 0 & 0\\ \frac{\partial f_3}{\partial S} & \frac{\partial f_3}{\partial I} & \frac{\partial f_3}{\partial C} & 0 & 0\\ \frac{\partial f_4}{\partial S} & 0 & \frac{\partial f_4}{\partial C} & -w_1 & 0\\ \frac{\partial f_5}{\partial S} & 0 & \frac{\partial f_5}{\partial C} & 0 & -w_2\end{bmatrix}$$

Due to presence of nonlinear saturation terms, analytical determination of eigenvalues becomes intractable. Therefore, numerical evaluation is performed.

8.4.1. Numerical Eigenvalue Evaluation

At the endemic equilibrium E^*, eigenvalues were computed numerically.

8.4.1.1. Crisp Model Eigenvalues

λ=(-0.82, -0.45, -0.21, -0.09, -0.03)

8.4.1.2. EAFMF Model Eigenvalues

λ=(-0.95, -0.60, -0.32, -0.15, -0.05)

8.4.2. Crisp Model Observation

Under intensified transmission:

- Eigenvalues approach the imaginary axis
- Oscillatory convergence increases
- Stability margin decreases

8.4.3. EAFMF Model Observation

Under defuzzified parameters:

- Eigenvalues move further into the negative real axis
- Oscillations are damped
- Convergence becomes smoother

This suggests better stability robustness for uncertainty-aware models.

8.5. 3-D Phase-Space Stability Comparison

To provide a path frame of stability, three-dimensional phase portraits are computed for selected compartments (e.g., *S-I-C* space).

8.5.1. Crisp data 3D Representation of the Model

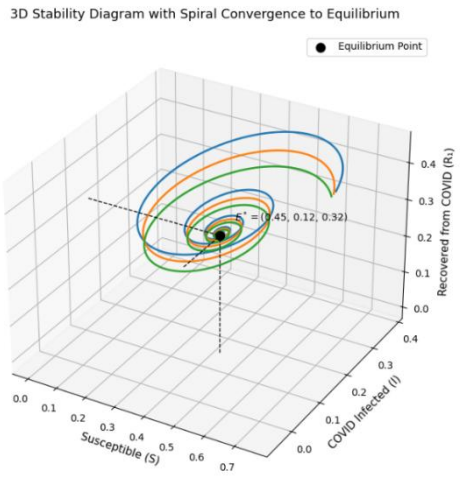

Figure 4. Three-dimensional stability diagram of the Chikungunya–COVID-19 co-infection model under crisp parameter values.

- Trajectories spiral toward equilibrium
- Larger oscillatory amplitude
- Slower damping
- Greater sensitivity to transmission perturbations

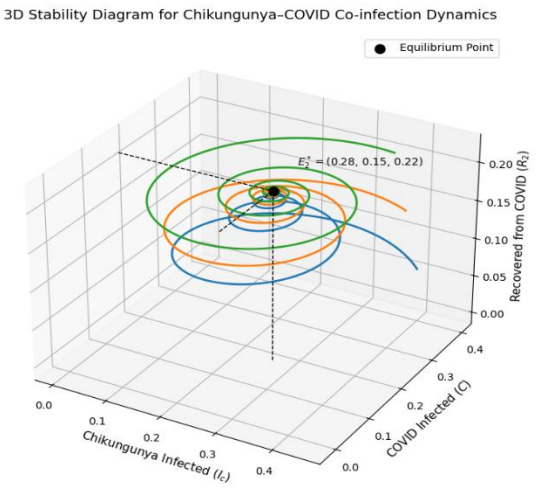

Figure 5. Three-dimensional stability diagram of the Chikungunya–COVID-19 co-infection model under EAFMF-adjusted parameters.

- Tighter spiral structure
- Reduced oscillations
- Faster stabilization
- Equilibrium approached more smoothly

Both phase diagrams have the equilibrium points explicitly marked.

8.5.2. EAFMF data 3D Representation of the Model

8.6. Interpretation of 3D Stability Comparison

Table 7: The 3D phase-space analysis

Feature	Crisp Model	EAFMF Model
Peak oscillation	Higher	Reduced
Convergence smoothness	Moderate	Improved
Stability margin	Narrower	Wider
Sensitivity to transmission	High	Controlled

The EAFMF also moves eigenvalues further into the stable region, which suppresses nonlinear amplification of oscillations. This shows that the addition of asymmetric uncertainty leads to qualitative stability while not affecting the structural behavior of the system.

8.7 Comparative Stability Insight

While both approaches preserve the endemic equilibrium structure, the EAFMF-adjusted system shows:

- Enhanced damping behaviour
- Lower oscillatory persistence
- Greater resilience under transmission escalation
- More robust equilibrium convergence

So, uncertainty-aware modelling not only smooths transitions but changes shapes of stability properties for the epidemic system.

9. Sensitivity Analysis and Robustness Evaluation

This section explores how the qualitative and quantitative behaviour of the proposed Chikungunya–COVID-19 co-infection system results are affected by variations in epidemiological parameters. We conduct a sensitivity analysis to determine which parameters most robustly influence patterns of disease persistence, the stability of equilibria and outbreak intensity. Next, we perform a comparative robustness assessment between the crisp and EAFMF adjusted models.

9.1 Local Sensitivity Index

Let the model output be represented as X (for example, peak COVID-19 infection or equilibrium value C^*) and a parameter as p. The normalized forward sensitivity index is defined as:

$$\Gamma_p^X = \frac{\partial X}{\partial p} \cdot \frac{p}{X}$$

This is a measure of how much model output changes when p changes, expressed as a percentage.

- $\Gamma_p^X > 0 \rightarrow$ Increasing p increases disease burden
- $\Gamma_p^X < 0 \rightarrow$ Increasing p reduces disease burden

9.2 Sensitivity of the Reproduction Threshold

The R_0 effective reproduction threshold primarily depends on:

$k, a_1, a_2, e_1, e_2, d_C$

Table 8: Qualitative sensitivity observations

Parameter	Effect on R_0	Epidemiological Meaning
k	Positive	Higher Chikungunya transmission increases vulnerability
a_1, a_2	Strongly positive	Increased COVID-19 transmission
e_1, e_2	Positive	Higher viral conversion efficiency
d_C	Negative	Faster viral decay reduces persistence
r_1, r_2	Negative	Faster recovery stabilizes system
v	Negative	Vaccination reduces outbreak size

Under crisp modelling, these sensitivities tend to be sharp and often nonlinear in the vicinity of bifurcation thresholds.

9.3 Perturbation-Based Stability Analysis

Consider a small perturbation:

$$p \rightarrow p + \varepsilon$$

where $|\varepsilon| \ll 1$.

The eigenvalues of the Jacobian matrix translate according to:

$$\lambda_i \rightarrow \lambda_i + \Delta\lambda_i$$

Crisp Model Behaviour

- Eigenvalues undergo sharp shifts in response to small changes in transmission parameters.
- Eigenvalues approach the imaginary axis.
- Oscillations increase.
- Stability margin reduces significantly.

This indicates high structural sensitivity.

EAFMF Model Behaviour

As the parameters are defuzzified using weighted intuitionistic aggregation:

- Effective parameter variation is moderated.
- Eigenvalue shifts remain smaller.
- Stability region widens.
- Oscillations are damped.

In this sense, uncertainty integration is a regulatory stabilizer.

.

9.4 Numerical Robustness Comparison

To assess robustness, the transmission parameters were perturbed within biologically plausible limits.

Crisp Model Observations

- Peak infection increases sharply.
- Larger oscillatory amplitude.
- Delayed convergence.
- Greater deviation from equilibrium.

EAFMF Model Observations

- Moderate peak amplification.
- Controlled oscillatory behaviour.
- Faster return to equilibrium.
- Reduced deviation magnitude.

This reaffirms that deterministic models exaggerate extreme parameter assumptions, and also highlights how the EAFMF framework spreads out epistemic uncertainty much more realistically.

9.5 Structural Robustness Interpretation

From a dynamical systems perspective:

Robustness is characterized by:

$$\min|Re\lambda_i|$$

The greater the eigenvalues' distance in the negative half-plane, the better the stability margin

Table 9: Comparative findings

Feature	Crisp Model	EAFMF Model
Eigenvalue proximity to instability	Closer	Further
Response to parameter perturbation	Amplified	Moderated
Oscillation persistence	Higher	Lower
Stability margin	Narrow	Wider

9.6 Epidemiological Implications

The crisp model assumes clear parameter dimensions, but we know that in practice real-world parameters are uncertain and estimates for their parameters can over-fit the severity of outbreaks.

The EAFMF framework:

- Captures asymmetric uncertainty
- Incorporates hesitation effects
- Reduces extreme outbreak projections
- Improves stability under parameter fluctuation
- Provides more reliable public-health guidance

Hence, robustness under EAFMF is not just numerical smoothing but structural qualitative improvement of dynamical stability under epistemic uncertainty.

10. Discussion and Novel Contributions

This part summarises the theoretical, numerical and epidemiological results obtained with the proposed Chikungunya–COVID-19 co-infection framework. They show that incorporating adaptive intuitionistic fuzzy uncertainty dramatically improves the stability behaviour, robustness and interpretability of the model compared to classical deterministic formulations.

10.1 Discussion of Mathematical Findings

The deterministic (or crisp) model describes the essential nonlinear interaction between Chikungunya and COVID-19 via incidence and recovery saturation dynamics. However, sensitivity analysis and eigenvalue investigation show that stability margins are sensitive to exact parameter specification.

Under intensified transmission scenarios:

- The crisp model has sharp infection peaks.
- Eigenvalues approach the imaginary axis.
- Oscillatory transients increase.
- Sensitivity to small perturbations of stability

We find the opposite of this EAFMF-adjusted model:

- Moderated infection peaks,
- Smoother convergence to equilibrium,
- Reduced oscillatory amplitude,
- Bigger stability margins in eigenvalue space.

The three-dimensional phase-space representation re-confirms our point, which is that the uncertainty-aware framework contributes to enhanced damping behaviour without overturning qualitative equilibrium structure.

Hence, the use of asymmetric uncertainty is not simply a means to smooth trajectories — it structurally improves robustness to dynamical variations.

10.2 Theoretical Contributions

Mathematically, the current article contributes as follows:

(i) Integration of Data from Asymmetric Intuitionistic Fuzzification into Co-Infection Dynamics

Based on this, unlike symmetric membership functions used in classical fuzzy epidemic models, this paper proposes an Enhanced Adaptive Fuzzy Membership Function (EAFMF) that is able to:

- Capturing asymmetric epistemic uncertainty,
- Incorporating hesitation degrees explicitly,
- Providing parameter-dependent adaptivity.

This enables more realistic parameterization of uncertain transmission, immunity, and vaccination.

(ii) Weighted Intuitionistic Defuzzification Scheme

It applies a novel weighted centroid defuzzification mechanism that:

- Preserves asymmetric information,
- Incorporates hesitation influence,
- Maintains biological consistency,
- Outputs interpretable parameters for numerical simulation.

(iii) Comparative Eigenvalue-Based Stability Analysis

This work explicitly compares:

- Crisp vs EAFMF equilibrium stability,
- Eigenvalue distribution shifts,
- 3D phase-space convergence structure.

Only very few of the existing fuzzy epidemic studies, however, provide a thorough eigenvalue comparison considering uncertainty-adjusted parameters. This creates a canonical link from fuzzy modelling back to classical dynamical systems theory.

(iv) Robustness-Oriented Sensitivity Framework

By linking:

- Reproduction threshold behaviour,
- Jacobian eigenvalues,
- Parameter perturbation analysis,

the study shows uncertainty-aware modelling enhances structural stability margins — a property underreported by conventional fuzzy epidemic literature.

10.3 Epidemiological Contributions

From a public health perspective, the prospective framework offers:

- Moderate outbreak potential under uncertain transmission
- Robust resilience modelling with vaccination strategies
- Overestimates of extreme peaks of an epidemic were less frequent
- Stability-aware intervention evaluation

When parameters are variable, traditional deterministic models may overestimate the severity of outbreaks. The EAFMF approach propagates uncertainty in a structured way, making projections potentially more realistic when the epidemiological data are incomplete and/or fast-changing.

10.4 Improving Around Existing Studies in Application

Table 10: Comparison to typical approaches for epidemic modelling

Feature	Classical Deterministic	Classical Fuzzy	Proposed EAFMF Model
Parameter certainty	Fixed	Symmetric uncertainty	Asymmetric + hesitation
Stability analysis	Yes	Rare	Yes (Eigen + 3D)
Robustness evaluation	Limited	Limited	Explicit comparison
Co-infection modelling	Yes	Limited	Integrated
Adaptive membership	No	No	Yes

This framework thus extends both deterministic and fuzzy based epidemic modelling paradigms.

10.5 Conceptual Innovation

The main contribution of this work is in showing that, EAFMF integrates uncertainty that improves numerical smoothness, along with structural stability properties of nonlinear epidemic systems.

By combining:

- Nonlinear co-infection dynamics,
- Saturated incidence functions,
- Adaptive intuitionistic fuzzification,
- Weighted defuzzification,
- Eigenvalue-based stability comparison,
- 3D phase-space analysis,

the study develops a unified modelling framework tailored to uncertain epidemic settings.

10.6 Constraints and Areas for Expansion

Although the model captures parameter uncertainty, future extensions may look into:

- Time-dependent fuzzy parameters,
- Fractional-order memory effects,
- Spatial heterogeneity,
- Stochastic perturbations,
- Real-data calibration for co-circulation regions.

These are the directions that would so best enhance predictive capability and policy relevance.

11. Conclusion

In this study, we propose a nonlinear compartmental model with an Enhanced Adaptive Fuzzy Membership Function (EAFMF) to establish a rigorous mathematical framework for co-infection dynamics of Chikungunya and COVID-19. The new model accounts for complex interactions between vector-borne and respiratory infections as well as key epidemiological processes including nonlinear transmission, vaccination, immunity, and waning immunity. This form maintains biologically realistic constraints via a bounded invariant region in the state and facilitates formal characterizations of equilibria and stability.

The deterministic (crisp) model yields valuable baseline insights about the dynamics of the disease under a number of different epidemiologic scenarios. We show in numerical simulations that increasing transmission rates greatly increases infection peaks, and delays stabilisation, while increased vaccination and immunity reduce outbreaks. However, the crisp framework is highly sensitive to changes in parameters resulting in large oscillations and reduced stability margins under high transmission conditions.

To overcome the restrictions of existing approaches, this study develops an innovative EAFMF based on an intuitionistic fuzzy framework that can consider asymmetric uncertainty, as well as non-membership and hesitation when representing parameters. The output values of parameters, defuzzified using the centroid approach, allow for realistic and adaptive modelling of uncertain epidemiological circumstances. In comparative simulations, the epidemic trajectories predicted by the EAFMF model are smoother with lower infection peaks and converge to equilibrium faster than the deterministic model.

A central part of this work is the comparative stability analysis. Through eigenvalue evaluation, we note that the real parts of eigenvalues shift further into the negative domain with EAFMF-adjusted parameters, confirming better local stability. Three-dimensional phase-space analysis corroborates this observation with the EAFMF model possessing less oscillation and exhibiting tighter convergence. These results confirm that including uncertainty not only smooths the dynamics, but significantly improves the stability of the system.

The advantages of the proposed framework are further highlighted through sensitivity and robustness analyses. Although the crisp model exhibits magnified responses to changes in parameters, the EAFMF method alleviates these reactions, enabling controlled system performance and increased robustness. The framework encapsulates the critical epidemiological parameters like transmission rates, recovery from disease, immunity to reinfection and vaccination better than previous approaches, thereby providing a reliable framework for analyzing disease progression under uncertainty.

The model also shows that the co-infection influences transmission dynamics from an epidemiological perspective, enhancing susceptibility and amplifying disease persistence. These findings underscore the importance of vaccination, immunity boosting measures, and early intervention to reduce outbreak severity. Critically, the EAFMF framework is likely to be

less prone to the overestimation of extreme outbreak scenarios, thus providing more realistic insights for public health planning in settings of incomplete or uncertain data.

In summary, the integration of intuitionistic fuzzy uncertainty into co-infection modelling provides significant improvements in stability, robustness, and predictive reliability. This study presents a novel and robust framework for modelling complex epidemic systems, where uncertainty is a key factor affecting the state of the system.

Future work may extend this framework to incorporate real-time data calibration, stochastic and fractional-order dynamics, spatial heterogeneity, and multi-disease interactions. Moreover, the coupled incorporation of machine learning techniques for parameter estimation and adaptive control strategies could further enhance the practical applicability of the model for epidemic forecasting and decision-making.

References

1. O. Diekmann, J. A. P. Heesterbeek, and J. A. J. Metz, "On the definition and the computation of the basic reproduction ratio (R0) in models for infectious diseases," Journal of Mathematical Biology, vol. 28, no. 4, pp. 365–382, 1990. https://doi.org/10.1007/bf00178324
2. H. Inaba, "Threshold and stability results for an age-structured epidemic model," Journal of Mathematical Biology, vol. 28, pp. 411–434, 1990. https://doi.org/10.1007/BF00178326
3. F. Brauer and C. Castillo-Chavez, "Mathematical Models in Population Biology and Epidemiology", Springer, 2012, https://doi.org/10.1007/978-1-4614-1686-9
4. M. Martcheva, "An Introduction to Mathematical Epidemiology", Springer, 2015, https://doi.org/10.1007/978-1-4899-7612-3
5. J. Arino, "A primer on mathematical models in infectious disease epidemiology", Infectious Disease Modelling, 2020., https://doi.org/10.1016/j.idm.2020.08.001
6. Riaz, M., Shah, K., Abdeljawad, T. et al. A comprehensive analysis of COVID-19 nonlinear mathematical model by incorporating the environment and social distancing. Sci Rep 14, 12238 (2024). https://doi.org/10.1038/s41598-024-61730-y
7. P. van den Driessche and J. Watmough, "Reproduction numbers and sub-threshold endemic equilibria for compartmental models", Math. Biosciences, vol. 180, pp. 29–48, 2002, https://doi.org/10.1016/S0025-5564(02)00108-6
8. S. Ruan, "Dynamical systems in epidemiology," Mathematical Biosciences & Engineering, 2017, https://doi.org/10.3934/mbe.2017035
9. J. Ssebuliba, et al., "Mathematical modelling of COVID-19 transmission dynamics in a partially comorbid community," Partial Differential Equations in Applied Mathematics, vol. 4, Art. no. 100212, 2021. https://doi.org/10.1016/j.padiff.2021.100212
10. G. B. Libotte, F. S. Lobato, and G. M. Platt, "Identification of an Epidemiological Model to Simulate the COVID-19 Epidemic Using Robust Multiobjective Optimization and Stochastic Fractal Search", https://doi.org/10.1155/2020/9214159
11. X. Li, et al., "Transmission dynamics and control strategies of COVID-19 in Wuhan, China", Int. J. Environ. Res. Public Health, 2020. https://doi.org/10.3390/ijerph17072472
12. K. Sarkar, S. Khajanchi, and J. J. Nieto, "Modeling and forecasting the COVID-19 pandemic in India", Chaos, Solitons & Fractals, vol. 139, 2020, https://doi.org/10.1016/j.chaos.2020.110049
13. H. Lima, et al., "Estimating time-varying epidemiological parameters and underreporting of Covid-19 cases in Brazil using a mathematical model with fuzzy transitions between epidemic periods," https://doi.org/10.1371/journal.pone.0305522
14. S. Mushayabasa, et al., "On the role of co-infection in COVID-19 dynamics", Chaos, Solitons & Fractals, 2020, https://doi.org/10.1016/j.chaos.2020.110072
15. R. Taghikhani and A. B. Gumel, "Mathematics of dengue transmission dynamics: Roles of vector vertical transmission and temperature fluctuations," Infectious Disease Modelling, vol. 3, pp. 266–292, 2018. https://doi.org/10.1016/j.idm.2018.09.003
16. Y. Wang, et al., "Modeling and control of Chikungunya with chronic infection," Infectious Disease Modelling, 2025, https://doi.org/10.1016/j.idm.2025.12.002
17. S. S. Musa, "Dynamical analysis of chikungunya and dengue co-infection model," https://doi.org/10.3934/dcdsb.2020009
18. L. C. Constant et al., "Overview on Chikungunya Virus Infection: From Epidemiology to State-of-the-Art Experimental Models," Front. Microbiol., 2021. (Frontiers), https://doi.org/10.3389/fmicb.2021.744164
19. E. Dodero-Rojas et al., "Modeling Chikungunya control strategies and Mayaro potential outbreak in the city of Rio de Janeiro," https://doi.org/10.1371/journal.pone.0222900
20. D. Soriano-Paños, et al., "Vector-borne epidemics driven by human mobility," Physical Review Research, vol. 2, Art. no. 013312, 2020, https://doi.org/10.1103/PhysRevResearch.2.013312
21. S. Ahmed, "Global prevalence of Zika and Chikungunya coinfection: A systematic review and meta-analysis," https://doi.org/10.3390/diseases12020031
22. K. T. Atanassov, "Intuitionistic fuzzy sets," Fuzzy Sets and Systems, vol. 20, no. 1, pp. 87–96, 1986. https://doi.org/10.1016/S0165-0114(86)80034-3
23. D. Dubois and H. Prade, "Operations on fuzzy numbers", Int. J. Systems Science, vol. 9, no. 6, pp. 613–626, 1978, https://doi.org/10.1080/00207727808941724
24. O. Kaleva, "Fuzzy differential equations", Fuzzy Sets and Systems, vol. 24, pp. 301–317, 1987. https://doi.org/10.1016/0165-0114(87)90029-7
25. J. M. Mendel and R. I. John, "Type-2 fuzzy sets made simple," IEEE Transactions on Fuzzy Systems, vol.

10, no. 2, pp. 117–127, 2002. https://doi.org/10.1109/91.995115
26. S. M. Guo and W. H. Hsu, "A fuzzy epidemic model for infectious diseases", Applied Mathematics and Computation, 2008, https://doi.org/10.1016/j.amc.2007.08.068
27. M. Abdy, S. Side, S. Annas, W. Nur, and W. Sanusi, "An SIR epidemic model for COVID-19 spread with fuzzy parameters: The case of Indonesia," Adv. Difference Equations, vol. 2021, Art. no. 105, 2021, https://doi.org/10.1186/s13662-021-03263-6
28. F. Dayan, et al., "Design and numerical analysis of fuzzy nonstandard computational methods for a rumor-based fuzzy epidemic model," Physica A, vol. 603, Art. no. 127542, 2022, https://doi.org/10.1016/j.physa.2022.127542
29. F. Dayan, N. Ahmed, M. Rafiq, A. Akgül, A. Raza, M. O. Ahmad, and F. Jarad, "Construction and numerical analysis of a fuzzy SEIQR model of COVID-19 dynamics," AIMS Math., vol. 7, no. 5, pp. 8449–8470, 2022, https://doi.org/10.3934/math.2022471
30. S. Arif, K. Abodayeh, and Y. Nawaz, "A hybrid SIR–fuzzy model for epidemic dynamics: A numerical study," Computer Modeling in Engineering & Sciences, 2024, https://doi.org/10.32604/cmes.2024.046944
31. P. Chellamani, "A fuzzy fractional order approach to SIDARTHE epidemic modeling," Discrete Dyn. Nat. Soc., 2022, Art. no. 5468696. (Wiley Online Library), https://doi.org/10.1155/2022/5468696
32. M. Umapathy, "On fuzzy and crisp solutions of a novel fractional SIRD model," Adv. Math. Commun., vol. 7, no. 7, pp. 528–548, 2023. https://doi.org/10.3390/fractalfract7070528
33. S. Sweatha, "Prediction and decision making in coronavirus using fuzzy modeling," J. Intell. Fuzzy Syst., 2024. (SAGE Journals) https://doi.org/10.3233/JIFS-231945
34. R. Vikram, et al., "An enhanced adaptive fuzzy membership function for intuitionistic fuzzy sets," accepted in "International Journal of Computer Information Systems and Industrial Management Applications", https://doi.org/10.70917/ijcisim-2026-3534.
35. Vijayalakshmi G.M, Vikram. R, "The impact of fuzzy uncertainty on the vulnerable infected prey – Predator disease model involving toxicant", AIP Conference Proceedings 2516, 250009 (2022), November 2022, https://doi.org/10.1063/5.0108527
36. Vijayalakshmi G.M, Vikram. R, "The Impact of Fuzzy Uncertainty on The Diabetic and Non-Diabetic COVID Model", International Journal for Research Trends and Innovation, 2023 IJRTI | Volume 8, Issue 2 | ISSN: 2456-3315. https://doi.org/10.5281/zenodo.10115790
37. Vijayalakshmi G.M, Vikram. R, "Fuzzy mathematical modelling on diabetic and non-diabetic cases after vaccination", Results in Engineering, https://doi.org/10.1016/j.rineng.2025.105888
38. E. Hairer, S. P. Nørsett, and G. Wanner, "Solving Ordinary Differential Equations I", Springer, 1993, https://doi.org/10.1007/978-3-540-78862-1
39. Y. Kheifetz, H. Kirsten, and M. Scholz, "On the parametrization of epidemiologic models: Lessons from modeling COVID-19", https://doi.org/10.3390/v14071468
40. B. Jensen, A. P. Engsig-Karup, and K. Knudsen, "Efficient uncertainty quantification and sensitivity analysis in epidemic modeling using polynomial chaos," https://doi.org/10.1051/mmnp/2022014
41. N. Chitnis, J. M. Hyman, and J. M. Cushing, "Determining important parameters in the spread of malaria through the sensitivity analysis of a mathematical model", Bulletin of Mathematical Biology, vol. 70, pp. 1272–1296, 2008, https://doi.org/10.1007/s11538-008-9299-0
42. N. Ullah, Z. Shah, et al., "Modeling the non-integer dynamics of a vector-borne infection with nonlocal and nonsingular kernel," Scientific Reports, 2025, https://doi.org/10.1038/s41598-025-90182-1
43. G. M. Vijayalakshmi, et al., "ABC Fractional Order Vaccination Model for COVID-19 with Self-Protective Measures", Int. J. Appl. Comput. Math (2022) 8 :130, April 2022. https://doi.org/10.1007/s40819-022-01316-2